ANNALS OF GEOPHYSICS, 69, 5, S554, 2026; doi:10.4401/ag-9555
OPEN ACCESS

Deep shear wave velocity model of the Venice lagoon from seismic noise interferometry

Ilaria Barone[*,1], Silvia De Marchi[1], Piero Poli[1], Jacopo Boaga[1]

(1) University of Padua, Department of Geosciences, Padova, Italy

Article history: received March 10, 2026; accepted July 28, 2026

Abstract

To establish a robust reference framework for future seismic hazard evaluations, we introduce the first deep shear wave velocity (Vs) model of the Venice Lagoon (Italy), developed through seismic noise interferometry. A seismometer was deployed in Venice's historic center, and its continuous noise recordings were cross-correlated with data from the sole permanent station located on Lido Island. Using seismic noise processing methods and joint inversion of Rayleigh wave group and phase velocity dispersion curves, we obtained a detailed deep Vs profile of the Venice Lagoon subsurface, extending down to the engineering bedrock and the base of the Pliocene sequence. Our model shows strong consistency with geological information from deep boreholes and seismic reflection surveys. Additionally, the determined engineering bedrock depth corresponds well with existing models of the deep alluvial Po Plain from earlier research. This study delivers the first comprehensive deep Vs reference model for Venice, establishing an essential baseline for future seismic response assessments and risk mitigation initiatives designed to safeguard the city's priceless cultural heritage.

Keywords: Venice Lagoon; Seismic Velocities; Passive Seismic Interferometry

1. Introduction

The historic city of Venice in north-eastern Italy represents an irreplaceable UNESCO cultural heritage site facing multiple natural hazards, including recurrent flooding (Zanchettin et al., 2021), subsidence (Carbognin et al., 2005) to the notable seismic hazard (Stucchi et al., 2011). Although Venice is far from active seismogenic faults, the region experiences significant seismic activity from surrounding areas (Burrato et al., 2008). A notable example occurred in 2012 when the M 6.1 Emilia Romagna earthquake sequence (Massa et al., 2012) was strongly felt in Venice's historic centre, causing minor damage to buildings and monuments despite an epicentral distance exceeding 90 km. Historical records document various earthquake impacts in the Venetian area (e.g., Galli, 2000; Carminati et al., 2007; Rovida et al., 2016), including the Verona earthquake of 1117 (estimated M 7), which damaged the city (Guidoboni et al., 2005). Although the seismic hazard is moderate, the exceptionally high levels of vulnerability and exposure substantially increase the overall seismic risk (Knezic et al., 2014), which requires adequate preparation and mitigation measures.

Understanding the response of the subsurface to dynamic forcing requires simulations of scenarios based on realistic geological models (Pitilakis, 2004; Pitilakis et al., 2006a, b; Sui, 2023). Seismic design codes (e.g., European Committee for Standardization, 2004; Ministero delle Infrastrutture e dei Trasporti, 2018; Building Seismic Safety

Council, 2020) typically require soil parameters obtained from direct investigations or geophysical surveys. However, due to logistical and financial constraints, mandatory characterization generally focuses only on shallow subsurface layers (Boore, 2004; Borcherdt, 2012). Conversely, comprehensive modeling scenarios and local seismic response assessments require deeper shear-wave velocity models extending to the seismic engineering bedrock (Borcherdt and Glassmoyer, 1992; Ambraseys et al., 1996; Kramer, 1996; Rathje et al., 2010) to realistically simulate the expected ground motions (Abrahamson and Silva, 1997).

Models reaching the rigid engineering bedrock (defined in European seismic codes as Vs ≥ 800 m/s, hereafter termed engineering bedrock) are therefore essential. However, in deep alluvial basins, the engineering bedrock can be found at considerable depths and remain inaccessible to conventional geophysical surveys (Guéguen et al., 2007). Consequently, various authors and seismic standards have proposed reference velocity structures that connect the upper subsurface to the depth of the engineering bedrock through linear or exponential gradients (Budny, 1984; Poggi et al., 2012; Faccioli et al., 2015; Cascone et al., 2022). Nevertheless, the depth of the engineering bedrock is often unknown (Mascandola et al., 2019), and this is exactly the case for Venice. Several studies have investigated the upper subsurface of Venice and its lagoon, primarily through shallow coring (Serandrei Barbero et al., 2001), providing detailed reconstructions and technical information on shallow subsurface layers (Zezza, 2010; Trevisani and Boaga, 2018; Simonini, 2023). Currently, deep geological reconstruction of the Venice area relies solely on a few continuous deep coring wells drilled during the 1970s (see Kent et al., 2002; Brambati et al., 2003; Massari et al., 2004), without any geophysical Vs measurements.

The Venice Lagoon presents a paradigmatic yet challenging environment for geophysical characterization of deep structures, as conventional extended seismic surveys cannot be conducted either at sea or on land. The shallow, semi-submerged wetlands prevent deployment of long seismic streamers, while protected natural park zones and historic centre logistics prohibit the use of conventional seismic sources (e.g., airgun or vibroseis). To overcome these limitations, we installed a seismometer in Venice and recorded ambient seismic noise for correlation with data from the only permanent seismic station in the Venice Lagoon located on Lido Island and part of the Italian National Seismic Network (Istituto Nazionale di Geofisica e Vulcanologia-INGV, 2005). This correlation forms the basis for seismic interferometry, a well-established and completely non-invasive technique enabling the extraction of the Green's function between sensor pairs (Weaver and Lobkis, 2004; Wapenaar, 2004; Shapiro and Campillo, 2004; Roux et al., 2005; Gouédard et al., 2008). The Green's function was then used for dispersion analysis and inversion to obtain the shear wave velocities of the medium studied (Mordret et al., 2015; Lehujeur et al., 2018; Kästle et al., 2018). This paper presents results from the first 3.5 months of noise monitoring. Our analysis enabled the definition of the deep shear wave velocity structure of the Venice Lagoon. The derived model agrees well with geological information from available deep boreholes in the area (CNR-VENEZIA 1; Favero et al., 1973; Massari et al., 2004) and studies of surrounding Po Plain zones (Boaga et al., 2010; Pesaresi et al., 2014; Mascandola et al., 2019), while additionally providing a Vs profile extending to the engineering bedrock of the Venice Lagoon and reaching the Basal discontinuity of the Pliocene. The identified discontinuity depth aligns with historical deep seismic reflection studies conducted in the surrounding areas of the Adriatic Sea and the Veneto Plains. This benchmark result establishes a crucial reference for future seismic response scenarios in Venice's historic centre.

Figure 1. Locations of the 2 seismometers in the Venice lagoon, North-East Italy. Black triangles show our San Servolo station and the Lido INGV station.

2. Data acquisition and preliminary analyses

In July 2023, we installed a seismometer on the Venetian Island of San Servolo (Fig. 1), home of the Venice International University (VIU). We used a triaxial Lunitek Tellus-5s seismometer, complemented by a Lunitek Atlas digital recorder and data transmission module. The instrument has a flat response in the frequency range of 0.3 to 100 Hz, with a dynamic range > 140 dB. The sampling frequency is set at 100 Hz. The instrument was placed in a temperature-controlled service room, basement level, on a rigid platform. The place is quiet, being off the main pathways of VIU attendants. The San Servolo station has been operating since 8 July 2023 and is currently the only one in the historic city of Venice. The nearest existing permanent station is located on the seafront, on the Lido Island (Fig. 1), and belongs to the Italian National Seismic Network IV, operated by the National Institute of Geophysics and Volcanology (INGV) with contributions from collaborating institutions and observatories (station code VENL). It is also a Lunitek Tellus-5s seismometer, coupled to a Lunitek ATLAS digital recorder, with a sampling frequency of 100 Hz. VENL (Lido) data are public and can be downloaded free of charge. The distance between our San Servolo station and the Lido station, as derived by GNSS, is 1629 m.

Preliminary analyses were carried out to assess the quality of the recorded data and the noise temporal stability. Figure 2a shows the spectrogram of the seismic noise recorded at San Servolo for the 0.1 Hz-5 Hz frequency range, using a 1-hour window. Five minor interruptions of recording can be easily identified, all of them lasting less than one day. The spectrogram allows us to appreciate the time distribution of noise in the different frequency ranges. The rather constant peak centred at 0.2 Hz corresponds to the secondary microseisms range, originated by the wave-wave interaction in the nearby oceans (Tanimoto and Anderson, 2023). The sparse peaks in the 0.3-1 Hz range are the effect of local wind-generated sea waves during storms, as demonstrated by the good correlation with the Adriatic sea wave height measurements taken in Ancona, at more than 200 km distance from our study site (Fig. 2b). The frequency of occurrence of these events in the period of analysis is rather stable, therefore no significant seasonal variations are observed. Finally, the regular daily pattern observed above 0.5 Hz with maximum amplitude around 1 Hz (see Figs. S1 and S2 in the Supplementary Information) corresponds to anthropic noise, probably due to maritime traffic and the consequent higher wave motion in the lagoon.

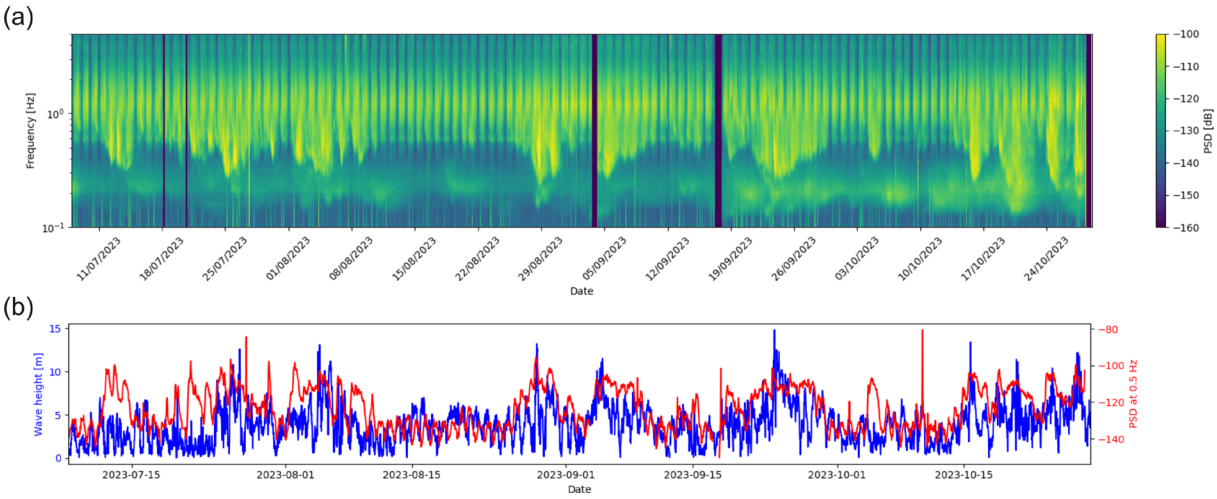

Figure 2. (a) Spectrogram of the seismic record in San Servolo for the period July 8, 2023 to October 28, 2023. (b) A horizontal slice of the spectrogram for 0.5 Hz (in red), and sea wave height recorded in Ancona for the same period. Very good correlation is observed between the two time series.

3. Methods

Seismic interferometry reconstructs the Earth's impulse response between receiver pairs through cross-correlation of ambient seismic noise (Wapenaar et al., 2010). Over recent decades, this passive technique has been extensively applied to retrieve Green's functions associated with virtual sources (Weaver and Lobkis, 2004; Roux et al., 2005;

Gouédard et al., 2008). This response is obtained by cross-correlating and stacking continuous passive recordings within a specific frequency range (Shapiro and Campillo, 2004). Green's function retrieval depends on either an isotropic azimuthal distribution of noise sources where noise wavefields aligned with the receiver pair contribute constructively while lateral wavefields produce destructive interference (Wapenaar et al., 2010), or on the predominance of inline noise sources. These conditions are rarely fully satisfied, so the obtained response is considered an approximation of the theoretical Green's function, termed the empirical Green's function (EGF; Shapiro and Campillo, 2004). Nevertheless, numerous studies have demonstrated that errors associated with non-uniform seismic source distributions are generally negligible when sufficiently long recordings are employed (Pedersen and Krüger, 2007; Yang and Ritzwoller, 2008; Weaver et al., 2009; Froment et al., 2010; Kästle et al., 2016).

Seismic interferometry can be expressed as (Weaver and Lobkis, 2004; Wapenaar, 2004; Shapiro and Campillo, 2004; Roux et al., 2005; Gouédard et al., 2008):

$$\{G(x_B, x_A, t) + G(x_B, x_A, -t)\} * S_N(t) = \langle u(x_B, t) * u(x_A, -t)\rangle \quad (1)$$

where from the ensemble averaging (⟨⟩) of the cross-correlations between signals recorded at station A (i.e., $u(x_A, t)$) and station B (i.e., $u(x_B, t)$), we can obtain the sum of the causal and acausal Green's functions between stations (i.e., $G(x_B, x_A, t)$ and $G(x_B, x_A, -t)$), convolved by the noise auto-correlation (i.e., S_N (t)). In this study the EGF was obtained by the following steps (Bensen et al., 2007; Poli et al., 2013): i) preprocessing raw time series, including resampling to 20 Hz and data demeaning; ii) segmenting continuous noise recordings into 1-hour time windows with 30-minute overlap; iii) applying spectral whitening to each data window by dividing the raw amplitude spectrum by its smoothed version (spectral normalization); iv) performing frequency-domain cross-correlation between records from the two analysed stations; v) stacking the cross-correlation spectra; vi) applying inverse Fourier transform to retrieve time-domain cross-correlations. Since this work focused on Rayleigh wave dispersion, cross-correlation of the vertical components of seismic traces (ZZ) was computed and analysed. The causal and acausal parts of the cross-correlation functions were averaged to compensate for imperfectly isotropic noise source distributions (Lin et al., 2008).

Rayleigh wave dispersion analysis was conducted both for group and phase velocities. The frequency time analysis (FTAN; Levshin et al., 1992; Boaga et al., 2010) was employed to identify the group velocity dispersion curve of surface waves from a single component and for the fundamental mode. The group velocity dispersion curve was first depth-inverted to obtain a preliminary 1D Vs model representing the average subsurface structure between San Servolo and Lido stations. Depth inversion was performed using the Dinver inversion code within the Geopsy package (https://www.geopsy.org/), that uses a stochastic approach based on the Neighborhood Algorithm (Sambridge, 1999; Wathelet, 2008). The parameter space for the inversion is shown in Table 1: target models include 5 layers with fixed density values and variable P- and S-wave velocities and thicknesses. Linear Vs gradients were permitted for the first three layers, while the deepest layers were constrained to uniform properties, a choice guided by the geological context of the deep sedimentary basin. The inversion was run using 100 starting models and brought to the generation of 20000 models in total.

Table 1. Parameter space for the group velocity inversion. Note that layers 1 to 3 admit a linear increase of Vs with depth, while for layers 4 and 5 Vs is constant.

Layer	Bottom depth [m]	*Vs* [m/s]	V_P [m/s]	ρ [kg/m^3]
1 (shallower)	100-500	150-500	300-1500	1800
2	250-1000	300-1300	600-3900	2000
3	600-1500	600-1500	1200-4500	2100
4	1200-2000	800-2000	1600-6000	2200
5	Inf	1200-2400	2400-7200	2400

To enhance depth resolution and obtain more robust Vs reconstruction, phase velocities were also extracted through analysis of the real part of the cross-spectrum (Aki, 1957; Pastén et al., 2016; Kästle et al., 2018; Barone et al., 2025). This method involves picking the most plausible phase velocities for all zero-crossing frequencies and requires a reference dispersion curve to guide low-frequency picking, overcoming the inherent uncertainty of phase velocity measurements at large distances. This reference curve was derived from the preliminary 1D Vs model obtained through group velocity inversion. Finally, the extracted group and phase velocity dispersion curves were jointly inverted to derive the final 1D Vs layered model of the subsurface extending to approximately 2 km depth. Joint depth inversion was also performed using Dinver with the same parameters as the group velocity inversion (Table 1). This model is considered more accurate than the preliminary model (derived from group velocities alone), particularly in its deeper portion, due to the increased depth sensitivity of phase velocities. Moreover, the integrated use of two independently derived datasets (group and phase velocities) makes the joint inversion result less susceptible to errors in dispersion analysis (Shapiro and Ritzwoller, 2002; Barone et al., 2024).

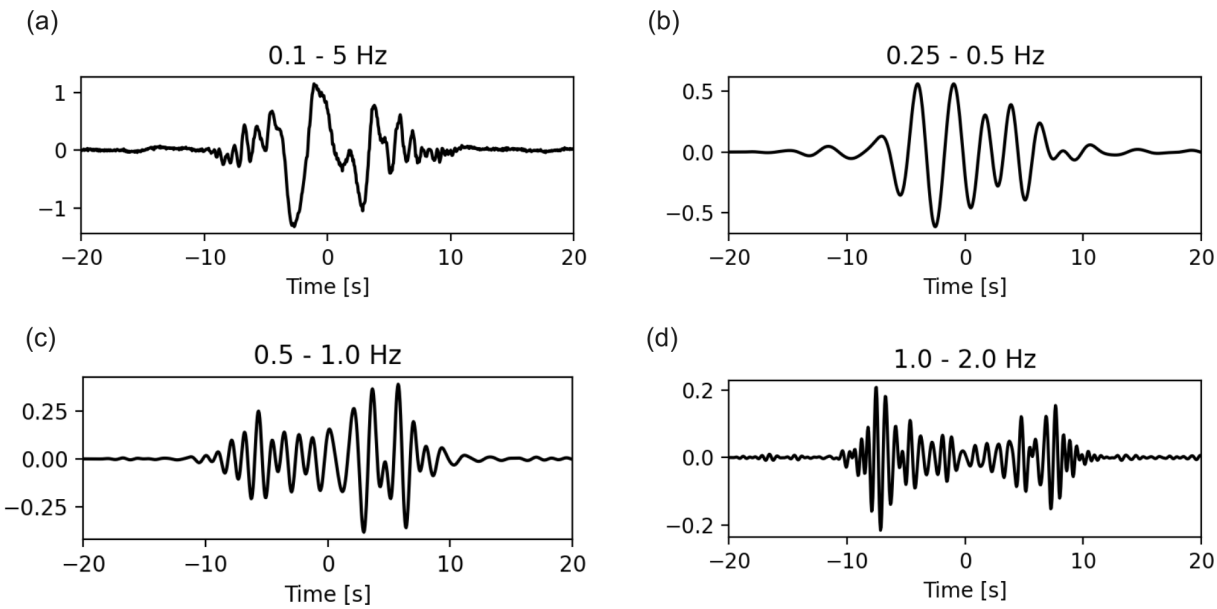

Figure 3. (a) EGF obtained through cross-correlation of the San Servolo and Lido stations, for the whole frequency band considered in this study (0.1-5 Hz), and bandpassed in the (b) 0.25-0.5 Hz, (c) 0.5-1.0 Hz and (d) 1.0-2.0 Hz frequency ranges. In all plots the casual (positive time lags) and acausal (negative time lags) parts represent the coherent noise propagating from Venice to Lido and from Lido to Venice, respectively.

4. Results

The data analysed here span the period from 8 July 2023 to 28 October 2023. The daily EGFs obtained from cross-correlation of San Servolo and Lido stations across the entire 0.1-5 Hz range show good consistency and no significant seasonal behaviour is observed (Fig. S3 in the Supplementary Information). A convergence analysis shows the stability of the EGF for increasing stacking lengths, and the expected increase of the signal-to-noise ratio (Fig. S4 in the Supplementary Information).

The final EGF obtained after stacking all daily EGFs for the period of analysis is shown in Fig. 3a. To better visualize the contribution of different frequency components, three different bandpass filters were applied (Figs. 3b-d). The almost symmetric character of the EGF in the different frequency ranges suggests a rather homogeneous distribution, although not perfectly isotropic, of the different noise source components.

The EGF resulting from averaging the causal and acausal parts, along with the FTAN spectrum, are presented in Fig. 4. The fundamental mode of Rayleigh waves is clearly recognizable between 0.3 Hz and 1.3 Hz, enabling manual velocity picking. At higher frequencies, multi-modal propagation is observed, complicating identification of the fundamental mode.

Figure 5 shows all the profiles generated by the inversion of the group velocity dispersion curve, with a different colour based on the misfit between observed and model dispersion curves. The dark blue model is the one that corresponds to the minimum misfit, i.e., the inverted model.

Figure 6a shows the real part of the cross-spectrum of the San Servolo-Lido station pair, while Fig. 6b shows all possible phase velocities associated with each zero-crossing frequency (blue points). The reference curve (in green), computed from the minimum misfit model in Fig. 5a, helps to identify the true phase velocities, which were manually sampled up to 2 Hz (red dots). Please note that the first zero-crossing was not considered since it gave unrealistic velocity values, too distant from the reference curve. This could be due to the reduced station distance with respect to the seismic wavelengths at these low frequencies.

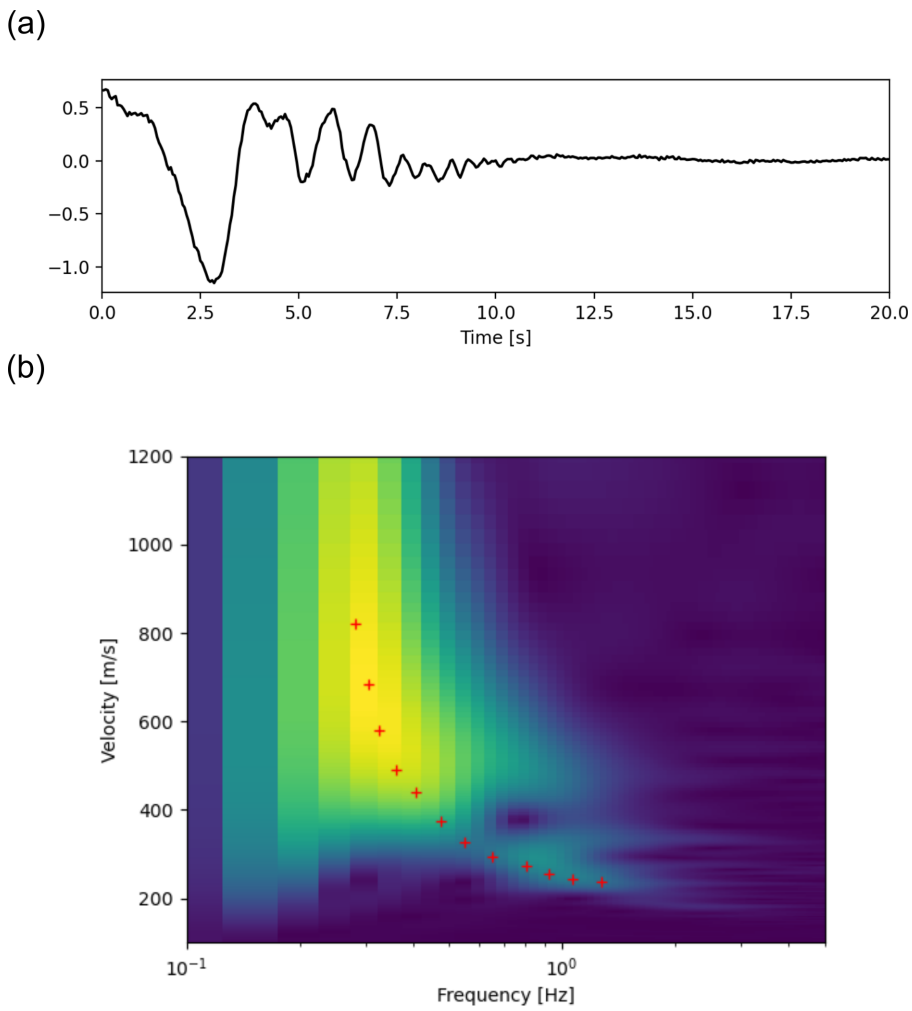

Figure 4. (a) EGF after averaging the causal and acausal parts. (b) Group velocity dispersion spectrum as derived by the FTAN technique. The curve was picked in the range 0.3-1.3 Hz. Rayleigh wave velocities show a clear decrease with frequency.

Results of the joint inversion of group and phase velocity dispersion curves are shown in Fig. 7. The best-fitting model (dark blue line in Fig. 7a) agrees with the preliminary model (Fig. 5a) in the shallow subsurface but shows some differences at greater depths. These differences arise from the greater depth sensitivity of phase velocities. Figure 8 illustrates the sensitivity kernels of both phase and group velocities at various frequencies, computed based on the model in Fig. 7a using the open-source Python library disba (Luu, 2021). At 0.3 Hz – the lowest frequency used in the joint inversion – phase velocities are sensitive to structures down to approximately 2 km depth, whereas group velocity sensitivity decays rapidly below 1.5 km. Given its ability to capture velocity variations across a broader depth range, we consider the Vs model obtained from the joint inversion as our preferred model.

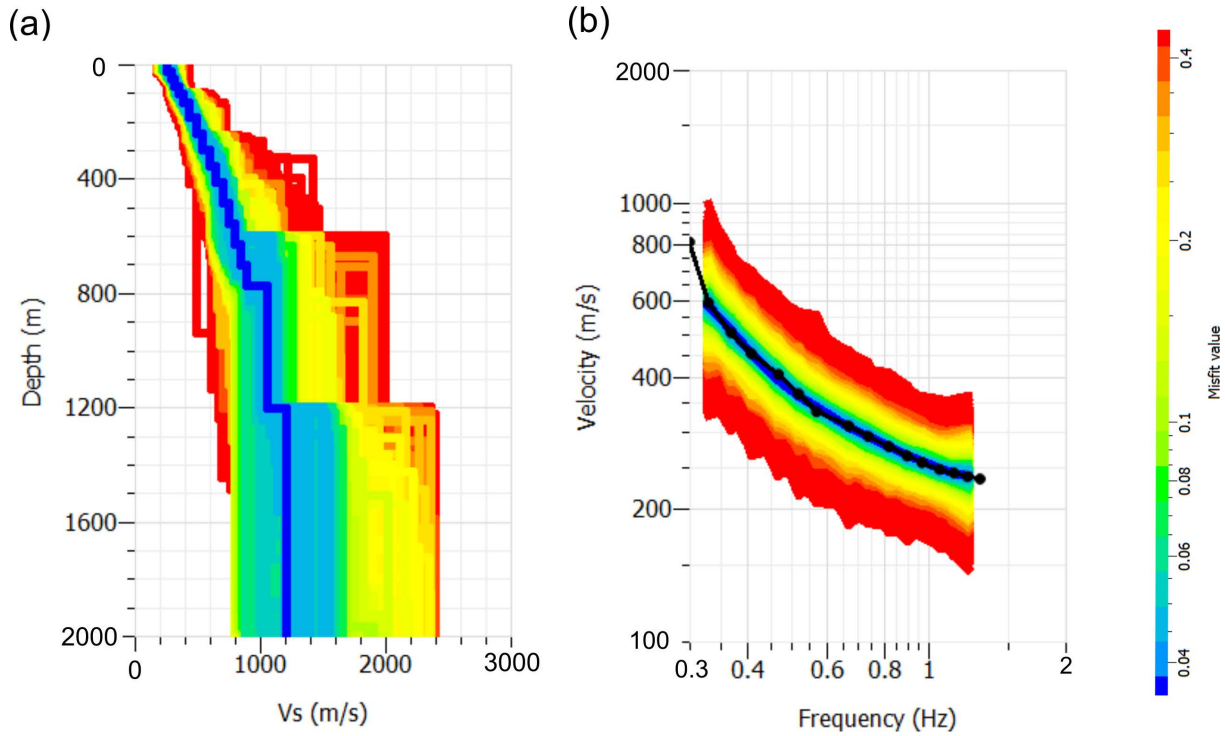

Figure 5. Results of the inversion of the group velocity dispersion curve obtained with FTAN: (a) Vs subsoil models generated by the stochastic inversion algorithm and (b) group velocity dispersion curves for the models in (a). The different colours indicate the inversion misfit. The observed dispersion curve is displayed in black. The dark blue model is the best fitting.

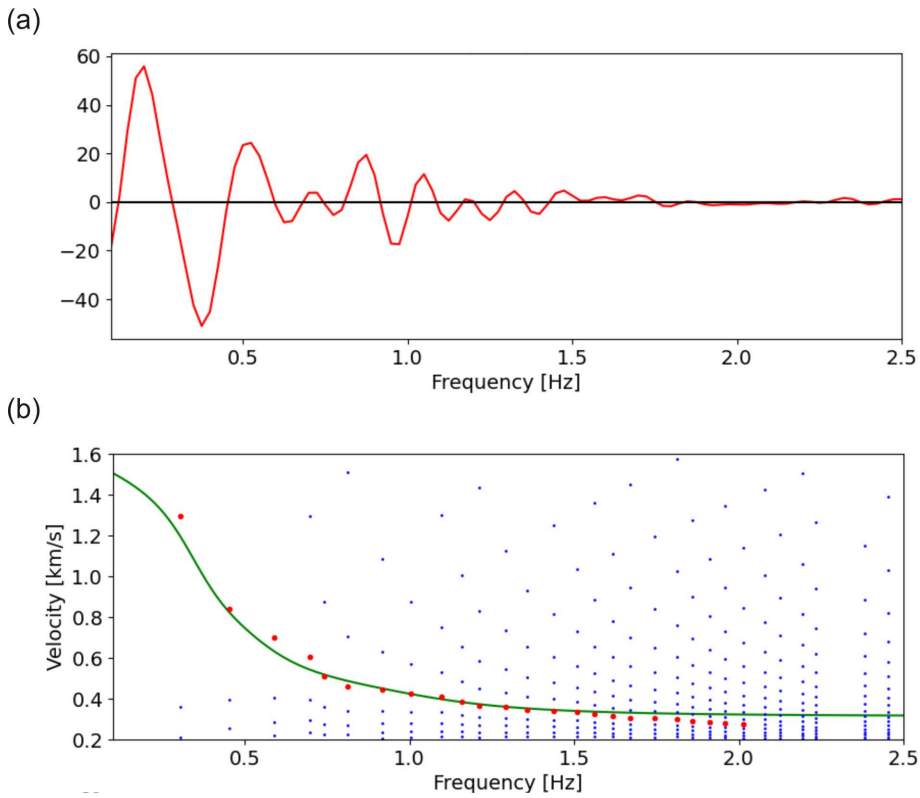

Figure 6. (a) Real part of the cross-spectrum. (b) Possible phase velocities associated with each zero-crossing frequency (blue dots) and picked velocities (red dots). The reference curve used to guide the picking is displayed in green (see Kästle et al., 2018).

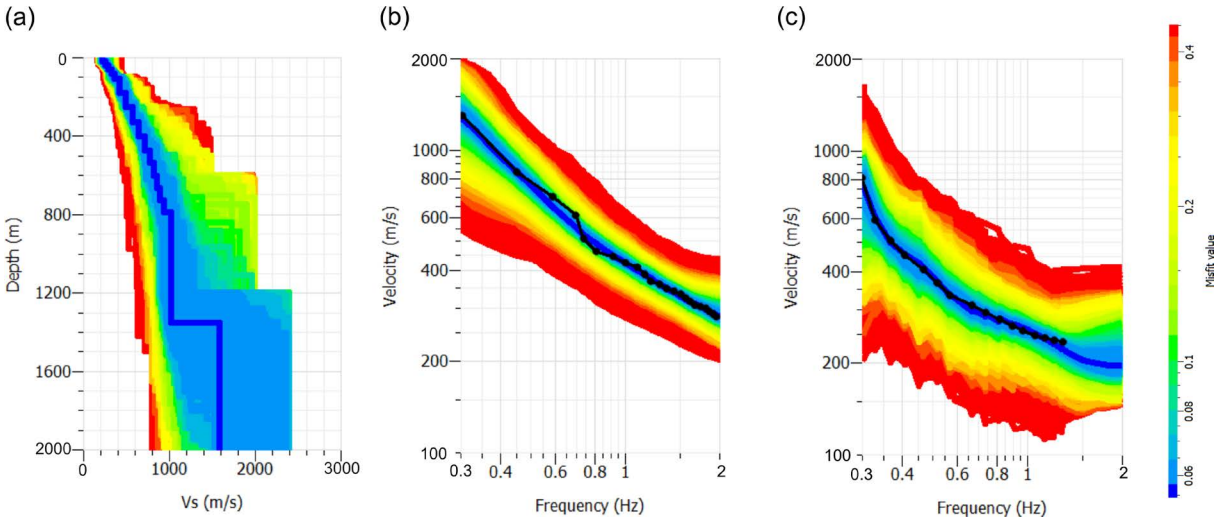

Figure 7. Result of the joint inversion of group and phase velocities for the studied area: (a) Vs subsoil models generated by the stochastic inversion algorithm; (b) phase velocity dispersion curves and (c) group velocity dispersion curves for the models in (a). The different colours indicate the inversion misfit. The observed dispersion curves are displayed in black. The dark blue model is the best fitting and represents our final Vs model.

5. Discussion

The installation of the first seismometer on one of the historic islands of Venice allowed reconstruction of the deep shear wave velocity structure of the Venetian lagoon subsoil by the use of ambient noise interferometry. A joint inversion of phase and group velocities was performed to increase the resolution in depth. The results are compared with the only existing deep boreholes drilled in the Venice Lagoon in the 1970s, the CNR-VE 1 and Lido 1 boreholes (Fig. 9). Despite the relevant amount of coring data, no borehole seismic data was collected and no seismic wave velocities were retrieved at that time. The CNR-VE 1 borehole was drilled to a depth of 950 m with continuous

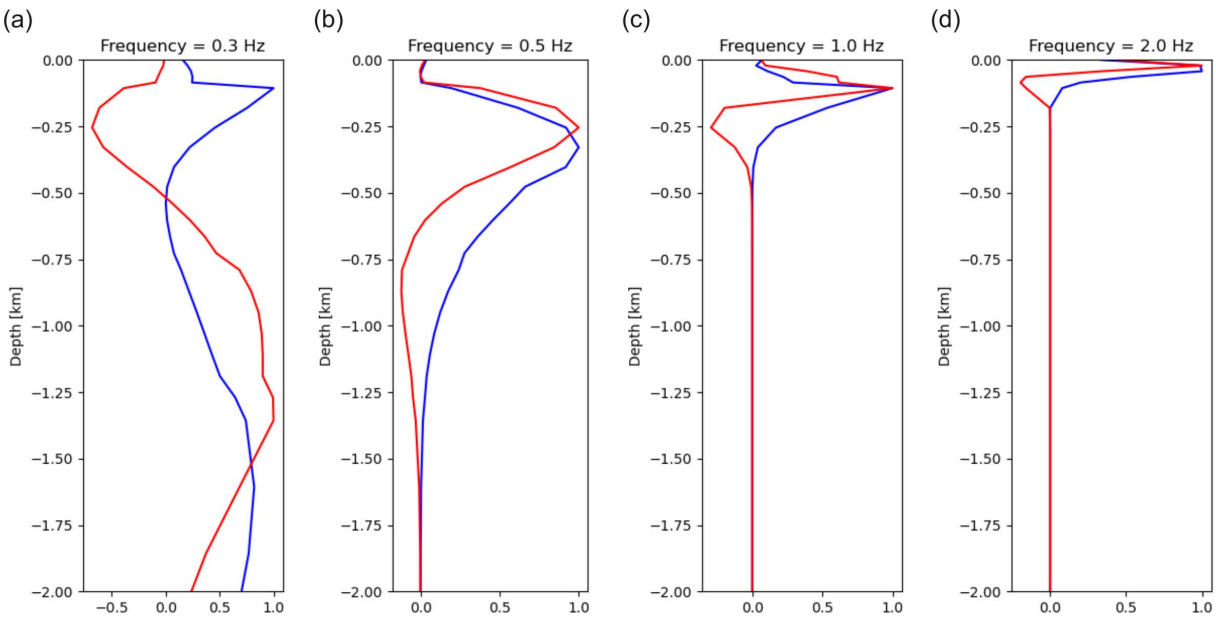

Figure 8. Normalized group velocity (red curve) and phase velocity (blue curve) Rayleigh wave sensitivity kernels for the frequencies (a) 0.3 Hz, (b) 0.5 Hz, (c) 1 Hz and (d) 2 Hz. Sensitivity kernels are relative to Vs and were computed based on the best fitting model in Fig. 6a.

coring, showing little variation with depth in terms of expected mechanical properties (Stefani et al., 2007), but rather a smooth continuous change due to lithostatic pressure alone. The Lido 1 borehole had very low recovery (Barbieri et al., 2007) but reached the Pliocene bottom unconformity at 1334 m depth. This represents the first major seismic reflector derived from seismic reflection surveys conducted for oil and gas purposes in the 1970s and 1980s (ENI, 1996). Figure 9 shows the depth of the bottom Pliocene surface derived from deep wells and seismic lines (Tosi et al., 2009, mod.), together with the seismic section of the closest deep reflection survey conducted in the region (Fantoni et al., 2002, mod.) and the two existing deep well stratigraphies (Barbieri et al., 2007, mod.). The shear-wave velocity model reconstructed with the ambient noise (dark blue line in Fig. 7a) agrees very well with these independent observations, highlighting a relevant velocity acceleration at ≈1350 m depth, most likely representing the bottom of the Pliocene. In fact, this is the main reflector observed in the old seismic sections and reached by the Lido 1 borehole at 1334 m (Fig. 9c).

From a seismic engineering perspective, our new Vs model suggests typical velocities for unconsolidated sediments down to a depth of ≈550 m (Fig. 7a). This level represents the seismic engineering bedrock (Vs ≥ 800 m/s, see European Committee for Standardization, 2004), suggesting a slightly deeper horizon than previous studies proposed in other Po plain sites by Pesaresi et al. (2014), Mascandola et al. (2019), and Cascone et al. (2022). In order to link the shallow subsoil profile with the engineering bedrock in the case of very deep alluvial plains or deep valleys, different

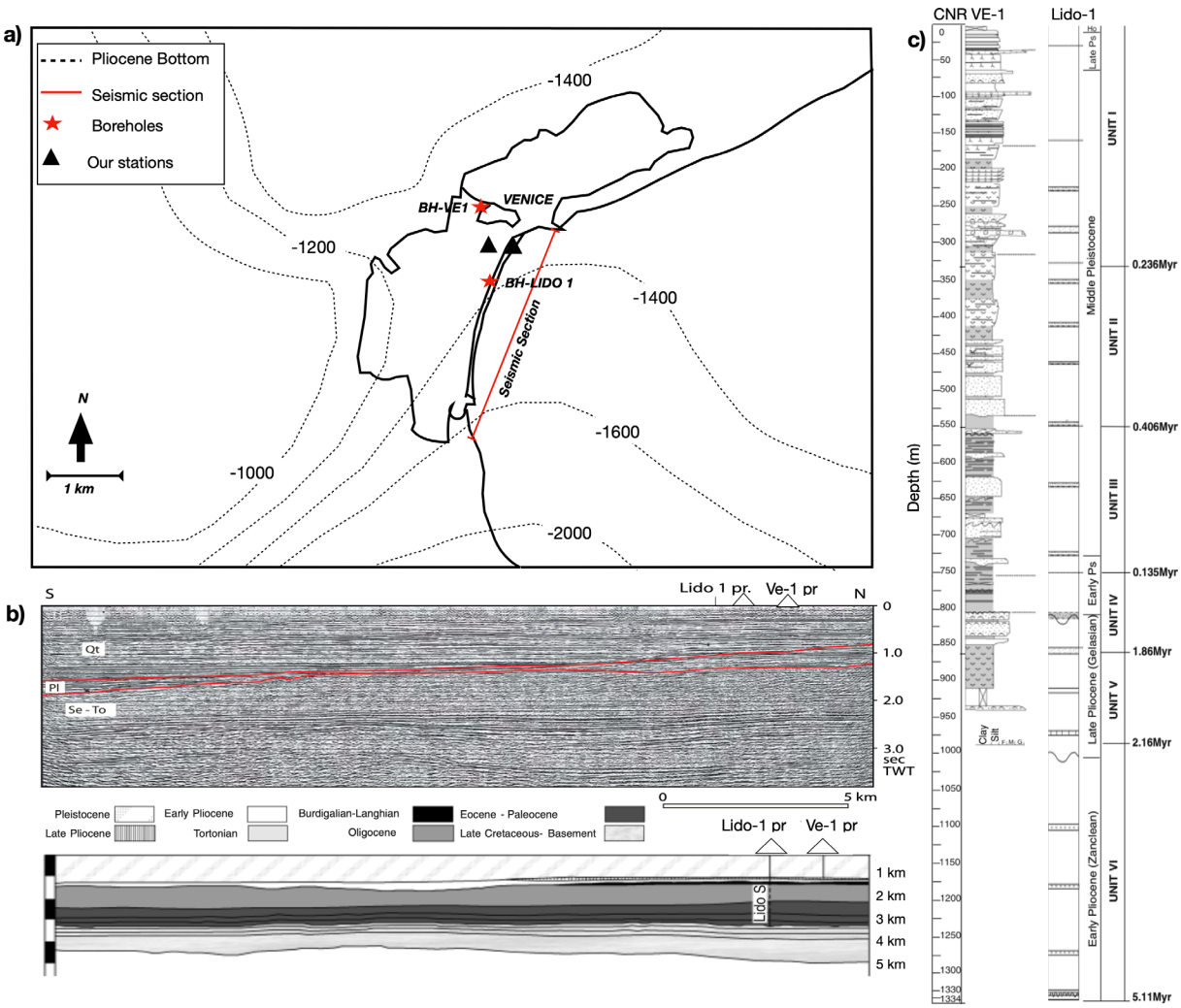

Figure 9. (a) Contour map representing the depth of the bottom Pliocene discontinuity in the Venice region (after Tosi et al., 2009, mod.), with the coastline represented with a continuous black line. (b) Closest deep available reflection seismic section (ENI 1996, mod.) and relative geological interpretation (in red roof and bottom of the Pliocene as in Barbieri et al.,2007, mod.) with the projected positions of the boreholes Lido 1 and CNR-VE 1; (c) Schematic stratigraphy from CNR-VE 1 and Lido 1 deep boreholes (after Stefani et al., 2006; Barbieri et al., 2007, mod.).

authors have proposed several velocity gradient laws, with a depth of engineering bedrock generally within 400 m depth (see Guéguen et al., 2007; Poggi et al., 2012). According to our experimental analysis, this value seems to be slightly deeper in the Venice Lagoon, characterized mainly by a very thick layer of soft sediments (Kent et al., 2002). As suggested in several seismic design standards, a linear gradient can be derived from a given Vs structure linking the shallow depth investigations reachable with common controlled source surveys (e.g., 30 m as in the Vs30 parameter) to the engineering bedrock. At the Venice site, a linear regression between 30 m depth and the engineering bedrock depth found in our best fit Vs model (550 m), suggests a linear gradient with depth (z) as in Eq. (2):

$$V_S(z) = 1.25\,z + 360 \tag{2}$$

For future seismic response scenarios involving the priceless historic centre of Venice, researchers and engineers can now rely on a measured depth of bedrock-like reference with Vs ≥ 800 m/s at a known depth, and adopt the suggested linear equation to connect their shallower structure to these deep horizons. The first subsoil needs to be characterized in fact site by site. Closer to the surface, the lagoon sediments are composed of soft sediments with different soil class velocities (Trevisani and Boaga, 2018). In this case study, the first few tens of meters are not properly resolved by the EGF study, as we relied only on low-frequency passive measurements. This suggests that careful local characterisation of the shallow subsurface, based on controlled-source techniques or local higher-frequency ambient noise methods, is still required for correct Vs30 estimate and seismic action design. A recent similar study for the characterisation of the Lido station area (group INGV, 2021) used a sparse array of 8 short-period seismometers recording 1 hour of ambient vibrations. A high-frequency phase velocity dispersion curve was extracted using the Extended Spatial Autocorrelation technique (ESAC; Okada and Suto, 2003). Figure 10 shows the comparison of this curve with the one obtained from our analysis of the cross-spectrum between the San Servolo and Lido stations. The good agreement in the common frequency range (1.5-2 Hz) further validates the proposed methodology for extracting phase velocities between station pairs. The small shift between the two curves is probably due to the very local nature of the ESAC curve, which is representative of the Lido site conditions (sandier than the lagoon part, Kent et al., 2002), and the high uncertainties of the ESAC technique at low frequencies due to the limited array size. Similar analyses can be performed to extend the phase velocity dispersion curve to higher frequencies and better constrain the model locally if needed.

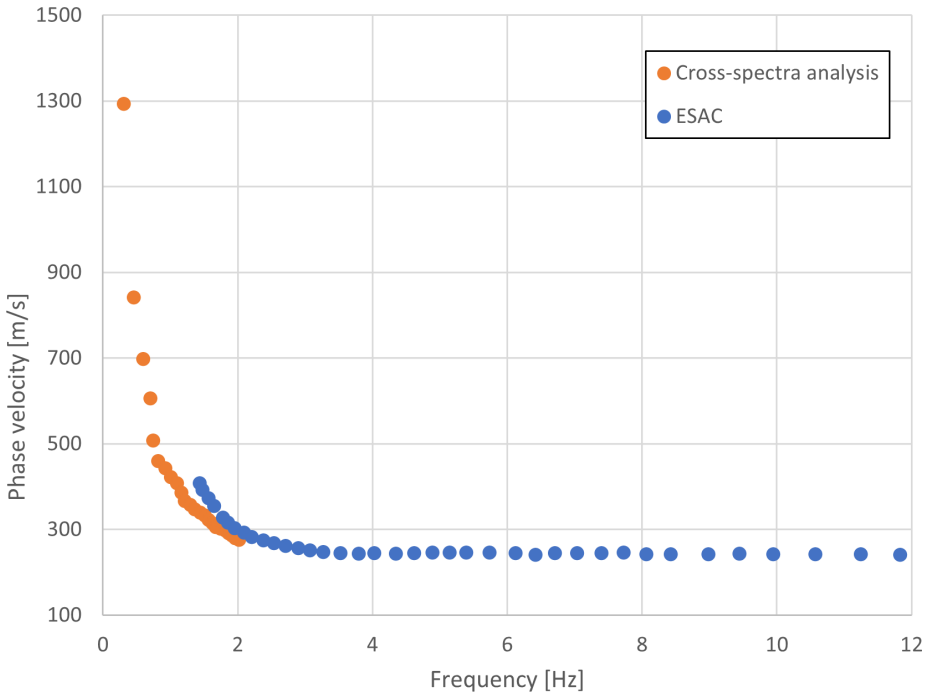

Figure 10. Comparison between the phase velocity dispersion curves obtained with the analysis of the cross-spectrum between San Servolo and Lido stations (orange), and the curve obtained by INGV with the ESAC method (blue).

6. Conclusions

We obtained the first deep subsurface characterisation of the Venice Lagoon using passive seismic interferometry. The aim was to provide the deep Vs structure down to the so-called engineering bedrock, to be adopted for more realistic seismic response scenarios for the protection of Venice's cultural heritage, a crucial information not yet known. In fact, while shallow geophysical investigations are common and mandatory for local seismic response analysis, a deep Vs model down to the engineering bedrock was missing for the Venice Lagoon. This is due to the particularly challenging conditions in the semi-submerged wetlands of the study area, which severely limit deep controlled-source seismic exploration. The use of passive interferometry, leveraging ambient seismic vibrations of both natural and anthropic origin, overcomes this limitation and provides the first characterisation of the deep structure of the Venice Lagoon. Our results are in agreement with the geological model as derived by deep coring and previous seismic reflection studies in the surrounding Venetian plain. The proposed study has defined the deep 1D Vs structure of the Venice Lagoon in a completely non-invasive way and represents a benchmark to be used as a reference for the future seismic response scenario of the historical centre of Venice. In the near future, the installation of more seismometers will allow cross-correlations between different station pairs to verify lateral heterogeneity and ultimately define a more accurate multi-dimensional deep model of the study area.

Data availability statement. The data underlying this article is publicly available in the Research Data Unipd archive at the link https://researchdata.cab.unipd.it/id/eprint/1856, doi.org/10.25430/researchdata.cab.unipd.it.00001856. The sea wave height series of Ancona can be downloaded from the ISPRA website (https://www.mareografico.it/it/stazioni.html).

Acknowledgements. Authors thank the Venice International University for the logistic support for seismometer installation, particularly Mr Igor Nash. The authors thank "The Geosciences for Sustainable Development" project (Budget Ministero dell'Università e della Ricerca – Dipartimenti di Eccellenza 2023-2027 C93C23002690001).

References

Abrahamson, N. A. and W. J. Silva (1997). Empirical Response Spectral Attenuation Relations for Shallow Crustal Earthquakes, Seismol. Res. Lett., 68, 94-127, doi:10.1785/gssrl.68.1.94.

Aki, K. (1957). Space and Time Spectra of Stationary Stochastic Waves, with Special Reference to Microtremors, Bull. Earthq. Res. Inst., 35, 415-456.

Ambraseys, N. N., K. A. Simpson and J. J. Bommer (1996). Prediction of Horizontal Response Spectra in Europe, Earthq. Eng. Struct. Dyn., 25, 371-400, doi:10.1002/(SICI)1096-9845(199604)25:4<371::AID-EQE550>3.0.CO;2-A.

Barbieri, C., A. Di Giulio, F. Massari, A. Asioli et al. (2007). Natural subsidence of the Venice area during the last 60 Myr, Basin Res., 19, 105-123, doi:10.1111/j.1365-2117.2007.00314.x.

Barone, I., A. Brovelli, G. Tango, S. Del Gaudio et al. (2025). Combined application of FTAN and cross-spectra analysis to ambient noise recorded by a microseismic monitoring network, Energy Geosci., 6, 100355, doi:10.1016/j.engeos.2024.100355.

Barone, I., V. Cascone, A. Brovelli, G. Tango et al. (2024). Shear-wave velocity structure derived from seismic ambient noise recorded by a small reservoir monitoring network, Geophys. Prospect., 72, 1789-1799, doi:10.1111/1365-2478.13486.

Bensen, G. D., M. H. Ritzwoller, M. P. Barmin, A. L. Levshin et al. (2007). Processing seismic ambient noise data to obtain reliable broad-band surface wave dispersion measurements, Geophys. J. Int., 169, 1239-1260, doi:10.1111/j.1365-246X.2007.03374.x.

Boaga, J., F. Vaccari and G. Panza (2010). Shear wave structural models of Venice Plain, Italy, from Time Cross Correlation of seismic noise, Eng. Geol., 116, 189-195, doi:10.1016/j.enggeo.2010.09.001.

Boore, D. M. (2004). Estimating Vs(30) (or NEHRP Site Classes) from Shallow Velocity Models (Depths < 30 m), Bull. Seismol. Soc. Am., 94, 591-597, doi:10.1785/0120030105.

Borcherdt, R. D. (2012). VS30 – A site-characterization parameter for use in building Codes, simplified earthquake resistant design, GMPEs, and ShakeMaps.

Borcherdt, R. D. and G. Glassmoyer (1992). On the characteristics of local geology and their influence on ground motions generated by the Loma Prieta earthquake in the San Francisco Bay region, California, Bull. Seismol. Soc. Am., 82, 603-641, doi:10.1785/BSSA0820020603.

Brambati, A., L. Carbognin, T. Quaia, P. Teatini et al. (2003). The Lagoon of Venice: geological setting, evolution and land subsidence, Episodes J. Int. Geosci., 26, 264-268, doi:10.18814/epiiugs/2003/v26i3/020.

Budny, M. (1984). Seismische Bestimmung der bodendynamischen Kennwerte von oberflaechennahen Schichten in Erdbebengebieten der Niederrheinischen Bucht und ihre ingenieurseismologische Anwendung, Geolog. Inst. d. Univ., Bibliothek.

Building Seismic Safety Council (2020). NEHRP Recommended Seismic Provisions for New Buildings and Other Structures (FEMA P-2082).

Burrato, P., M. E. Poli, P. Vannoli, A. Zanferrari et al. (2008). Sources of Mw 5+ earthquakes in northeastern Italy and western Slovenia: An updated view based on geological and seismological evidence, Tectonophysics, 453, 157-176, doi:10.1016/j.tecto.2007.07.009.

Carbognin, L., P. Teatini and L. Tosi (2005). Land Subsidence in the Venetian area: known and recent aspects, Giornale di Geologia Applicata, 1, 5-11, doi:10.1474/GGA.2005-01.0-01.0001.

Carminati, E., S. Enzi and D. Camuffo (2007). A study on the effects of seismicity on subsidence in foreland basins: An application to the Venice area, Global Planet. Change, 55, 237-250, doi:10.1016/j.gloplacha.2006.03.003.

Cascone, V., I. Barone and J. Boaga (2022). Velocity gradients choice affecting seismic site response in deep alluvial basins: Application to the Venetian Plain (Northern Italy), J. Geophys. Eng., 19, 1-13, doi:10.1093/jge/gxab067.

ENI (1996). Lineamento geologico minerario, Dominio subalpino orientale, report.

European Committee for Standardization (2004). Eurocode 8: Design of structures for earthquake resistance – Part 1: General rules, seismic actions and rules for buildings.

Faccioli, E., R. Paolucci and M. Vanini (2015). Evaluation of Probabilistic Site-Specific Seismic-Hazard Methods and Associated Uncertainties, with Applications in the Po Plain, Northern Italy, Bull. Seismol. Soc. Am., 105, 2787-2807, doi:10.1785/0120150051.

Fantoni, R., D. Catellani, S. Merlini, S. Rogledi et al. (2002). La registrazione degli eventi deformativi cenozoici nell'avampaese Veneto-Friulano, Mem. Soc. Geol. Ital., 57, 301-313.

Favero, V., L. Alberotanza and R. Serandrei Barbero (1973). Aspetti paleoecologici, sedimentologici e geochimici dei sedimenti attraversati dal pozzo VE 1 bis C.N.R., in Sondaggi profondi per lo studio della subsidenza: relazioni sul pozzo Venezia 1: 1. fase: operazioni di cantiere (Rapporto n. 63), C.N.R., Laboratorio per lo studio della dinamica delle grandi masse, Venezia, 1-51.

Froment, B., M. Campillo, P. Roux, P. Gouédard et al. (2010). Estimation of the effect of nonisotropically distributed energy on the apparent arrival time in correlations, GEOPHYSICS, 75, SA85-SA93, doi:10.1190/1.3483102.

Galli, P. (2000). New empirical relationships between magnitude and distance for liquefaction, Tectonophysics, 324, 169-187, doi:10.1016/S0040-1951(00)00118-9.

Gouédard, P., L. Stehly, F. Brenguier, M. Campillo et al. (2008). Cross-correlation of random fields: Mathematical approach and applications, Geophys. Prospect., 56, 375-393, doi:10.1111/j.1365-2478.2007.00684.x.

Guidoboni, E., A. Comastri and E. Boschi (2005). The "exceptional" earthquake of 3 January 1117 in the Verona area (northern Italy): A critical time review and detection of two lost earthquakes (lower Germany and Tuscany), J. Geophys. Res. Solid Earth, 110, doi:10.1029/2005JB003683.

Guéguen, P., C. Cornou, S. Garambois and J. Banton (2007). On the Limitation of the H/V Spectral Ratio Using Seismic Noise as an Exploration Tool: Application to the Grenoble Valley (France), a Small Apex Ratio Basin, Pure Appl. Geophys., 164, 115-134, doi:10.1007/s00024-006-0151-x.

Group INGV, W. (2021). Agreement DPC-INGV 2019-21, All. B2-WP1, Task 2. Site characterization report at the seismic station IV.VENL – Venezia Lido (VE).

Istituto Nazionale di Geofisica e Vulcanologia (INGV) (2005). Rete Sismica Nazionale (RSN), doi:10.13127/SD/X0FXNH7QFY.

Kent, D. V., D. Rio, F. Massari, G. Kukla et al. (2002). Emergence of Venice during the Pleistocene, Quat. Sci. Rev., 21, 1719-1727, doi:10.1016/S0277-3791(01)00153-6.

Knezic, S., M. Scudeller, M. Indirli, F. Romagnoli et al. (2014). The ANDROID Case Study; Venice and its Territory: Identification of Hazards and Impact of Multi-hazard Scenarios, Procedia Econ. Finance, 18, 465-472, doi:10.1016/S2212-5671(14)00964-2.

Kramer, S. L. (1996). Geotechnical Earthquake Engineering, Prentice Hall, Upper Saddle River, NJ.

Kästle, E. D., A. El-Sharkawy, L. Boschi, T. Meier et al. (2018). Surface Wave Tomography of the Alps Using Ambient-Noise and Earthquake Phase Velocity Measurements, J. Geophys. Res. Solid Earth, 123, 1770-1792, doi:10.1002/2017jb014698.

Kästle, E. D., R. Soomro, C. Weemstra, L. Boschi et al. (2016). Two-receiver measurements of phase velocity: cross-validation of ambient-noise and earthquake-based observations, Geophys. J. Int., 207, 1493-1512, doi:10.1093/gji/ggw341.

Lehujeur, M., J. Vergne, J. Schmittbuhl, D. Zigone et al. (2018). Reservoir imaging using ambient noise correlation from a dense seismic network, J. Geophys. Res. Solid Earth, 123, 6671-6686, doi:10.1029/2018JB015440.

Levshin, A., L. Ratnikova and J. Berger (1992). Peculiarities of surface-wave propagation across central Eurasia, Bull. Seismol. Soc. Am., 82, 2464-2493, doi:10.1785/BSSA0820062464.

Lin, F. C., M. P. Moschetti and M. H. Ritzwoller (2008). Surface wave tomography of the western United States from ambient seismic noise: Rayleigh and Love wave phase velocity maps, Geophys. J. Int., 173, 281-298, doi:10.1111/j.1365-246X.2008.03720.x.

Luu, K. (2021). Disba: Numba-accelerated computation of surface wave dispersion, Zenodo, doi:10.5281/ZENODO.5775195.

Massa, M., S. Lovati, D. Sudati, G. Franceschina et al. (2012). INGV strong-motion data web-portal: a focus on the Emilia seismic sequence of May-June 2012, Ann. Geophys., 55, doi:10.4401/ag-6120.

Mascandola, C., M. Massa, S. Barani, D. Albarello et al. (2019). Mapping the engineering bedrock of the Po Plain (Italy) through Ambient-Vibration Monitoring, Bull. Seismol. Soc. Am., 109, 164-177, doi:10.1785/0120180193.

Massari, F., D. Rio, R. Serandrei Barbero, A. Asioli et al. (2004). The environment of Venice area in the past two million years, Palaeogeogr. Palaeoclimatol. Palaeoecol., 202, 273-308, doi:10.1016/S0031-0182(03)00640-0.

Ministero delle Infrastrutture e dei Trasporti (2018). Decreto Ministeriale 17 gennaio 2018, Norme Tecniche per le Costruzioni (NTC 2018). Aggiornamento delle Norme tecniche per le costruzioni.

Mordret, A., D. Rivet, M. Landès and N. M. Shapiro (2015). Three-dimensional shear velocity anisotropic model of Piton de la Fournaise Volcano (La Réunion Island) from ambient seismic noise, J. Geophys. Res. Solid Earth, 120, 406-427, doi:10.1002/2014JB011654.

Okada, H. and K. Suto (2003). The Microtremor Survey Method, Geophysical Monograph Series, Society of Exploration Geophysicists, doi:10.1190/1.9781560801740.

Pastén, C., M. Sáez, S. Ruiz, F. Leyton et al. (2016). Deep characterization of the Santiago Basin using HVSR and cross-correlation of ambient seismic noise, Eng. Geol., 201, 57-66, doi:10.1016/j.enggeo.2015.12.021.

Pedersen, H. A. and F. Krüger (2007). Influence of the seismic noise characteristics on noise correlations in the Baltic shield, Geophys. J. Int., 168, 197-210, doi:10.1111/j.1365-246X.2006.03177.x.

Pesaresi, D., M. Romanelli, C. Barnaba, P. L. Bragato et al. (2014). OGS improvements in 2012 in running the North-eastern Italy seismic network: the Ferrara VBB borehole seismic station, Adv. Geosci., 36, 61-67, doi:10.5194/adgeo-36-61-2014.

Pitilakis, K. (2004). Site Effects, in A. Ansal (Editor), Recent Advances in Earthquake Geotechnical Engineering and Microzonation, Springer Netherlands, Dordrecht, 139-197, doi:10.1007/1-4020-2528-9_6.

Pitilakis, K., M. Alexoudi, S. Argryroudis and A. Anastasiadis (2006a). Seismic risk scenarios for an efficient seismic risk management: The case of Thessaloniki (Greece), in S.T. Wasti and G. Ozcebe (Editors), Advances in Earthquake Engineering for Urban Risk Reduction, Springer Netherlands, Dordrecht, 229-244, doi:10.1007/1-4020-4571-9_15.

Pitilakis, K., C. Gazepis and A. Anastasiadis (2006b). Design response spectra and soil classification for seismic code provisions, ETC-12 Geotechnical Evaluation and Application of the Seismic Eurocode EC8: Proceedings of the Athens Workshop, 37-52.

Poggi, V., D. Fäh, J. Burjanek and D. Giardini (2012). The use of Rayleigh-wave ellipticity for site-specific hazard assessment and microzonation: application to the city of Lucerne, Switzerland, Geophys. J. Int., 188, 1154-1172, doi:10.1111/j.1365-246X.2011.05305.x.

Poli, P., H. A. Pedersen, M. Campillo and the POLENET/LAPNET Working Group (2013). Noise directivity and group velocity tomography in a region with small velocity contrasts: the northern Baltic shield, Geophys. J. Int., 192, 413-424, doi:10.1093/gji/ggs034.

Rathje, E. M., A. R. Kottke and W. L. Trent (2010). Influence of Input Motion and Site Property Variabilities on Seismic Site Response Analysis, J. Geotech. Geoenviron. Eng., 136, 607-619, doi:10.1061/(ASCE)GT.1943-5606.0000255.

Roux, P., K. G. Sabra, W. A. Kuperman and A. Roux (2005). Ambient noise cross correlation in free space: Theoretical approach, J. Acoust. Soc. Am., 117, 79-84, doi:10.1121/1.1830673.

Rovida, A., M. Locati, R. Camassi, B. Lolli et al.(2016). Catalogo Parametrico dei Terremoti Italiani (CPTI15), versione 1.5, doi:10.6092/INGV.IT-CPTI15.

Sambridge, M. (1999). Geophysical inversion with a neighbourhood algorithm – I. Searching a parameter space, Geophys. J. Int., 138, 479-494, doi:10.1046/j.1365-246X.1999.00876.x.

Serandrei Barbero, R., A. Lezziero, A. Albani and U. Zoppi (2001). Late Pleistocene and Holocene deposits in the Venetian underground: Palaeo environments and history, Alpine Mediterr. Quat., 14, 9-22.

Shapiro, N. M. and M. Campillo (2004). Emergence of broadband Rayleigh waves from correlations of the ambient seismic noise, Geophys. Res. Lett., 31, doi:10.1029/2004GL019491.

Shapiro, N. M. and M. H. Ritzwoller (2002). Monte-Carlo inversion for a global shear-velocity model of the crust and upper mantle, Geophys. J. Int., 151, 88-105, doi:10.1046/j.1365-246X.2002.01742.x.

Simonini, P. (2023). Geology of the lagoon, in Geotechnics of Venice and Its Lagoon, CRC Press, p. 18.

Stefani, C., M. G. Fellin, M. Zattin, G. G. Zuffa et al. (2007). Provenance and Paleogeographic Evolution in a Multi-Source Foreland: The Cenozoic Venetian-Friulian Basin (NE Italy), J. Sediment. Res., 77, 867-887, doi:10.2110/jsr.2007.083.

Stucchi, M., C. Meletti, V. Montaldo, H. Crowley et al. (2011). Seismic Hazard Assessment (2003-2009) for the Italian Building Code, Bull. Seismol. Soc. Am., 101, 1885-1911, doi:10.1785/0120100130.

Sui, Y. (2023). A real-time approach to structural seismic response analysis, Soil Dyn. Earthq. Eng., 175, 108226, doi:10.1016/j.soildyn.2023.108226.

Tanimoto, T. and A. Anderson (2023). Seismic noise between 0.003 Hz and 1.0 Hz and its classification, Prog. Earth Planet. Sci., 10, 56, doi:10.1186/s40645-023-00587-7.

Tosi, L., P. Teatini, L. Carbognin and G. Brancolini (2009). Using high resolution data to reveal depth-dependent mechanisms that drive land subsidence: The Venice coast, Italy, Tectonophysics, 474, 271-284, doi:10.1016/j.tecto.2009.02.026.

Trevisani, S. and J. Boaga (2018). Passive seismic prospecting in Venice historical center for impedance contrast mapping, Environ. Earth Sci., 77, 733, doi:10.1007/s12665-018-7918-0.

Wapenaar, K. (2004). Retrieving the Elastodynamic Green's Function of an Arbitrary Inhomogeneous Medium by Cross Correlation, Phys. Rev. Lett., 93, 254301, doi:10.1103/PhysRevLett.93.254301.

Wapenaar, K., D. Draganov, R. Snieder, X. Campman et al. (2010). Tutorial on seismic interferometry: Part 1 – Basic principles and applications, GEOPHYSICS, 75, 75A195-75A209, doi:10.1190/1.3457445.

Wathelet, M. (2008). An improved neighborhood algorithm: Parameter conditions and dynamic scaling, Geophys. Res. Lett., 35, doi:10.1029/2008GL033256.

Weaver, R., B. Froment and M. Campillo (2009). On the correlation of non-isotropically distributed ballistic scalar diffuse waves, J. Acoust. Soc. Am., 126, 1817-1826, doi:10.1121/1.3203359.

Weaver, R. L. and O. I. Lobkis (2004). Diffuse fields in open systems and the emergence of the Green's function (L), J. Acoust. Soc. Am., 116, 2731-2734, doi:10.1121/1.1810232.

Yang, Y. and M. H. Ritzwoller (2008). Characteristics of ambient seismic noise as a source for surface wave tomography, Geochem. Geophys. Geosyst., 9, doi:10.1029/2007gc001814.

Zanchettin, D., S. Bruni, F. Raicich, P. Lionello et al. (2021). Sea-level rise in Venice: historic and future trends (review article), Nat. Hazards Earth Syst. Sci., 21, 2643-2678, doi:10.5194/nhess-21-2643-2021.

Zezza, F. (2010). The sedimentary structure of Upper Pleistocene Holocene deposits in Venice and its effects on the stability of the historic centre, Rend. Lincei, 21, 211-227.

***CORRESPONDING AUTHOR: Ilaria BARONE**,
University of Padua, Department of Geosciences, via Gradenigo 6, 35131 Padova, Italy
e-mail: ilaria.barone@unipd.it

© 2026 the Author(s).
Open Access. This article is licensed under a Creative Commons Attribution 4.0 International License